Flyback Forward Topology Based Three Port Dc-Dc Converter For Photovoltaic Systems

Rajeshkumar.G

PG Student

Department of EEE

Annai Vailankanni College of Engineering

Abstract- System efficiency and cost effectiveness are of critical importance for photovoltaic (PV) systems. This paper addresses the two issues by developing a novel three-port DC-DC converter for stand-alone PV systems, based on an improved Flyback-Forward topology. It provides a compact single-unit solution with a combined feature of optimized maximum power point tracking (MPPT), high step-up ratio, galvanic isolation and multiple operating modes for domestic and aerospace applications. The developed technology is capable of achieving MPPT, high conversion ratio and multiple operating modes whist still making the converter relatively simple, light, efficient and cost-effective. The project is focused on a comprehensive modulation strategy utilizing both PWM and phase-shifted control that satisfies the requirement of PV power systems to achieve MPPT and output voltage regulation. Simulation is conducted to analyze the usage of RLC load in the proposed converter.

KeyTerms **: DC-DC power conversion, maximum power pointp tracking, phase shift, photovoltaic power system, voltage control.**

1 INTRODUCTION

1.1 General

Solar energy is a primary and renewable source of energy. As the cost of photovoltaic (PV) panels is seen to reduce continuously, PV-based power generation is gaining in popularity for both grid-connected and stand-alone systems. Currently, the global installation is over 40 GW and increases at an annual rate of 50% since 2005. Stand-alone systems are independent of utility grids and commonly employed for satellites, space stations, unmanned aerial vehicles (UAV) and domestic applications. Such systems require storage elements to accommodate the intermittent generation of solar energy. Over the years, research effort has been directed toward improving the power conversion efficiency as well as the power density by weight (PDW) and the power density by volume (PDV).

Traditionally, the two-port topology utilizes the dual active bridges (DAB) and the half or full bridges can support the multiport structure to some extent. A combination of Flyback-Forward converter with full bridge has shown some advantages in zero voltage switching (ZVS) and high conversion ratio for fuel cell applications. A modified half bridge converter is reported in previous studies, which consists of one PV input port, one bidirectional battery port, and an isolated output for satellite applications. However, in these converters, a multi-input-multi-output (MIMO) solution is generally difficult to achieve for power electronic applications.

In theory, multiple-input converters (e.g. three-port converters) can provide a single-unit solution interfacing multiple energy sources and common loads. They perform better than traditional two-port converters due to their lower part count and smaller converter size. In particular, the isolated three-port converter (ITPC) has become an attractive topology for various applications owing to their multiple energy source connection, compact structure and low cost. In this topology, a simple power flow management scheme can be used since the control function is centralized. A high-frequency transformer can provide galvanic isolation and flexible voltage conversion ratio. The ITPC is usually integrated into an individual converter such as forward, push-pull, full bridge, and Flyback converters.

The ITPC utilizes the triple active bridges (TAB) with inherent features of power controllability and ZVS. Their soft-switching performance can be improved if two series-resonant tanks

are implemented. An advanced modulation strategy is incorporates a phase shift (PS) and a PWM to extend the operating range of ZVS. Nonetheless, the TAB topology suffers from the circuit complexity using three active full bridges or half bridges and the power loss caused by reactive power circulation.

1.2 Power Electronics

Power electronics is the application of solid-state electronics to the control and conversion of electric power. It also refers to a subject of research in electronic and electrical engineering which deals with the design, control, computation and integration of nonlinear, time-varying energy-processing electronic systems with fast dynamics.

The first high power electronic devices were mercury-arc valves. In modern systems the conversion is performed with semiconductor switching devices such as diodes, thyristors and transistors, pioneered by R. D. Middle brook and others beginning in the 1950s. In contrast to electronic systems concerned with transmission and processing of signals and data, in power electronics substantial amounts of electrical energy are processed. An AC/DC converter (rectifier) is the most typical power electronics device found in many consumer electronic devices, e.g. television sets, personal computers, battery chargers, etc.

1.5 DC-to-DC Converter

A DC-to-DC converter is an electronic circuit which converts a source of direct current (DC) from one voltage level to another. It is a class of power converter. DC to DC converters are important in portable electronic devices such as cellular phones and laptop computers, which are supplied with power from batteries primarily. Such electronic devices often contain several sub-circuits, each with its own voltage level requirement different from that supplied by the battery or an external supply (sometimes higher or lower than the supply voltage).

1.6 Application of Power Electronics

Applications of power electronics range in size from a switched mode power supply in an AC adapter, battery chargers, fluorescent lamp ballasts, through variable frequency drives and DC motor drives used to operate pumps, fans, and manufacturing machinery, up to gigawatt-scale high voltage direct current power transmission systems used to interconnect electrical grids. Power electronic systems are found in virtually every electronic device. For example:

- DC/DC converters are used in most mobile devices (mobile phones, PDA etc.) to maintain the voltage at a fixed value whatever the voltage level of the battery is. These converters are also used for electronic isolation and power factorcorrection. A power optimizer is a type of DC/DC converter developed to maximize the energy harvest from solar photovoltaic or wind turbine systems.

- AC/DC converters (rectifiers) are used every time an electronic device is connected to the mains (computer, television etc.). These may simply change AC to DC or can also change the voltage level as part of their operation.

2 LITERATURE REVIEW

1. Feel-Soon Kang, Sung-Jun Park, Su Eog Cho, Cheul-U Kim, and ToshifumiIse,"Multilevel PWM Inverters Suitable for the Use of Stand-Alone Photovoltaic Power Systems"this paper presents a new multilevel pulse width-modulation (PWM) inverter scheme for the use of stand-alone photovoltaic systems. It consists of a PWM inverter, an assembly of level inverters, generating staircase output voltages, and cascaded transformers. To produce high-quality output voltage waves, it synthesizes a large number of output voltage levels using cascaded transformers, which have a series-connected secondary. By a suitable selection of the secondary turn-ratio of the transformer, the amplitude of an output voltage appears at the rate of an integer to an input dc source. Operational principles and analysis are illustrated in depth.

2. Yen-Mo Chen, Alex Q. Huang, "A High Step-Up Three-Port DC–DC Converter for Stand-Alone PV/Battery Power Systems" this paper presents a three-port dc–dc converter integrating photovoltaic (PV) and battery power for high step-up applications. The topology includes five power switches, two coupled inductors, and two active-clamp circuits. The coupled inductors are used to achieve high step-up voltage gain and to reduce the voltage stress of input side switches. Two sets of active-clamp circuits are used to recycle the energy stored in the leakage inductors and to improve the system efficiency. The operation mode does not need to be changed when a transition between charging and discharging occurs. Moreover, tracking maximum power point of the PV source and regulating the output voltage can be operated simultaneously during charging/discharging transitions. As long as the sun irradiation level is not too low, the maximum power point tracking (MPPT) algorithm will be disabled only when the battery charging voltage is too high.

3. Fan Zhang, KaryThanapalan, Andrew Procter, Stephen Carr, and Jon Maddy, "Adaptive Hybrid Maximum Power Point Tracking Method for a Photovoltaic System" this paper presentsa novel hybrid maximum power point tracking mechanism with adaptive perturbation size. Recently, the importance of exploring the plausibility of renewable energy has been progressively increased, not only because of concerns over the shortage of current fossil fuels but also the consideration of sustainable development and the negative environmental impact caused by large scale use of fossil fuels. Among renewable sources, solar energy seems to be one of the promising energy sources for widespread application.

4. Haimin Tao, Andrew Kotsopoulos, Jorge L. Duarte and Marcel A. M. Hendrix "Transformer-Coupled Multiport ZVS Bidirectional DC–DC Converter with Wide Input Range"this paper presents a zero-voltage switching (ZVS) three-port bidirectional dc–dc converter. A simple and effective duty ratio control method is proposed to extend the ZVS operating range when input voltages vary widely. Soft-switching conditions over the full operating range are achievable by adjusting the duty ratio of the voltage applied to the transformer winding in response to the dc voltage variations at the port. Keeping the volt-second product (half-cycle voltage-time integral) equal for all the windings leads to ZVS conditions over the entire operating range. A detailed analysis is provided for both the two-port and the three-port converters. Furthermore, for the three-port converter a dual-PI-loop based control strategy is proposed to achieve constant output voltage, power flow management, and soft-switching. The three-port converter is implemented and tested for a fuel cell and super capacitor system.

5. Christos Konstantopoulos, EftichiosKoutroulis, "Global Maximum Power Point Tracking of Flexible Photovoltaic Modules" this paper describes the flexible Photovoltaic (PV) modules have the advantage of easily fitting on curved surfaces, but in that case their power-voltage characteristic exhibits local Maximum Power Points (MPPs) where the PV module power production is suboptimal. The effect of geometrical installation parameters of flexible PV modules, such as the bending angle, tilt angle and orientation, on the shape of the power-voltage characteristic is experimentally investigated. An experimental, comparative study is also presented, which demonstrates that compared to the past-proposed MPP tracking techniques, the system proposed in this paper is capable to detect the global MPP of a flexible PV module with less search steps. Thus, the power loss during the global MPP tracking process is minimized and the energy production of the flexible PV module is maximized

3 PROPOSED METHOD

An isolated three-port DC-DC converter for stand-alone PV systems, based on an improved Flyback-Forward topology is proposed. The converter can provide a high step-up capability for power conversion systems including the PV array, the battery storage, and the isolated load consumption. Three operating modes are analyzed and have shown the effective operation of the proposed topology for PV applications.

3.1 Topology and Operation

The proposed converter topology is illustrated in figures. The main switches $s_1$and $s_2$transfer the energy from the PV to the battery or load, and can work in either interleaved or synchronous mode. The switches $s_3$and $s_4$are operated in the interleaved mode to transfer energy from source to load. $L_1$and$L_2$are two coupled inductors whose primary winding (n_1) is employed as a filter and the secondary windings (n_2) are connected in series to achieve a high output voltage gain. $L_{LK}$is the leakage inductance of the two coupled inductors and *N* is the turns ratio from n_2/n_1. C_{s1}, C_{s2}, C_{s3} and C_{s4}, are the parasitic capacitors of the main switchess_1,s_2, s_3,and $s_4$respectively. There are three operational modes for the converter, as illustrated in Fig 3.2. In mode 1, the PV array supplies power to load and possibly also to the battery, corresponding to the daytime operation of the PV system.

Fig 3.4, where V_{GS1}, V_{GS2}, $V_{GS3}$and V_{GS4} are the gate drive signals, $V_{dS1}$and V_{dS2} are the voltage stresses of $s_1$and s_2, $i_{L1a}$and , $i_{L2a}$are the currents through $L1a$ and $L2a$, respectively. $i_B$is the current through the battery, $i_{s1}$is the current throughs_1, $v_{D_{01}}$is the voltage stress of the output diodeD_{01}, and $i_{D_{01}}$is the current through D_{01}.

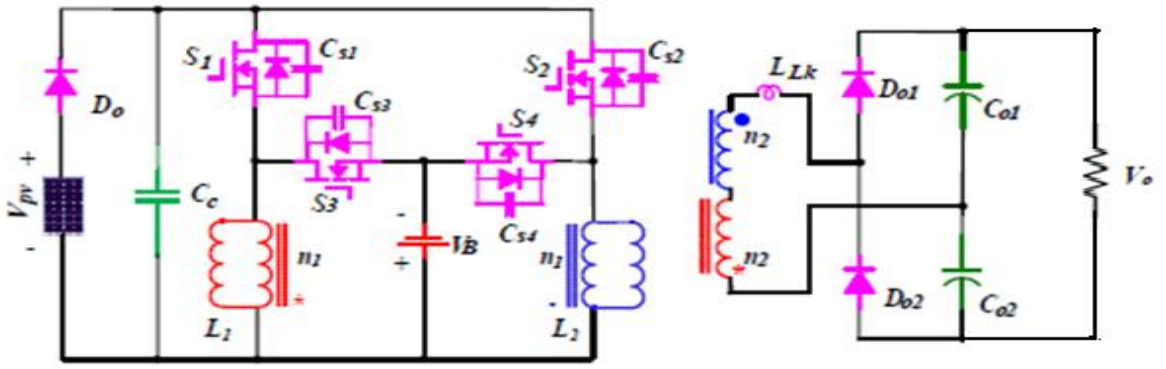

Figure 3.1: Proposed converter topology with resistive load

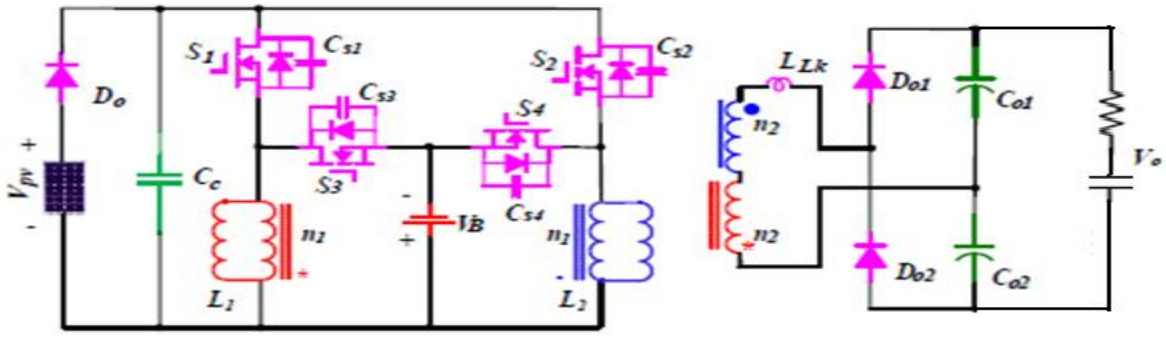

Figure 3.2 : Proposed converter topology with RC load

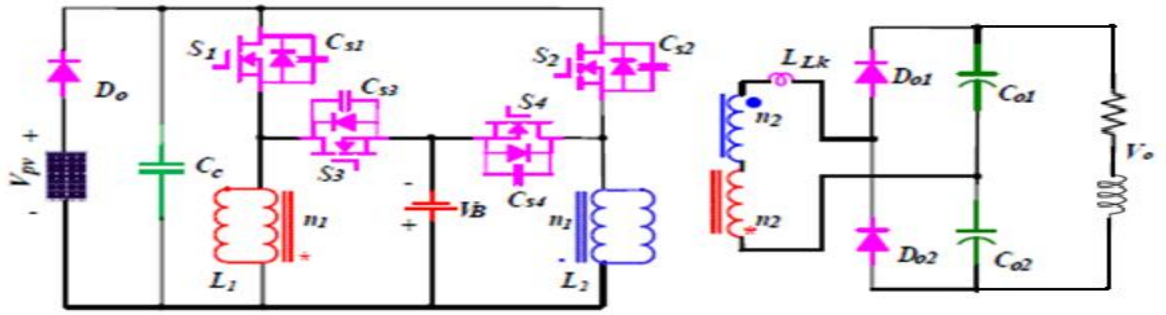

Figure 3.3 : Proposed converter topology with RL load

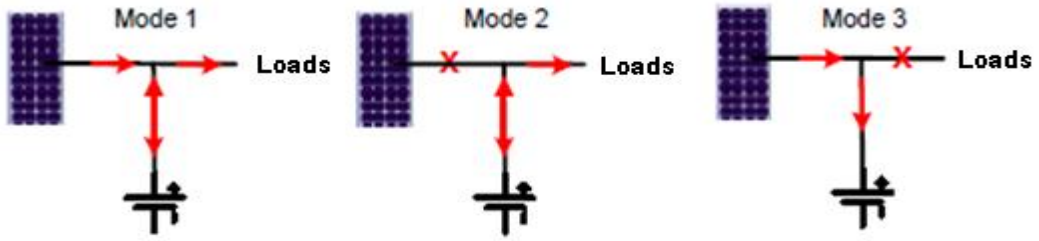

Figure 3.4: Three operation modes of the proposed converter

State 1 [t_0- t_1]:

The main switches$s_1$and $s_2$are both in turn-on state beforet_0. The two coupled inductors work in the flyback state to store energy from the PV array. The output rectifier diodes $D_{01}$and $D_{02}$are both reverse-biased. The energy stored in the secondary output capacitors $C_{01}$and C_{01}transfers to the load. A first operating state of the proposed converter in mode 1 is shown in figure.

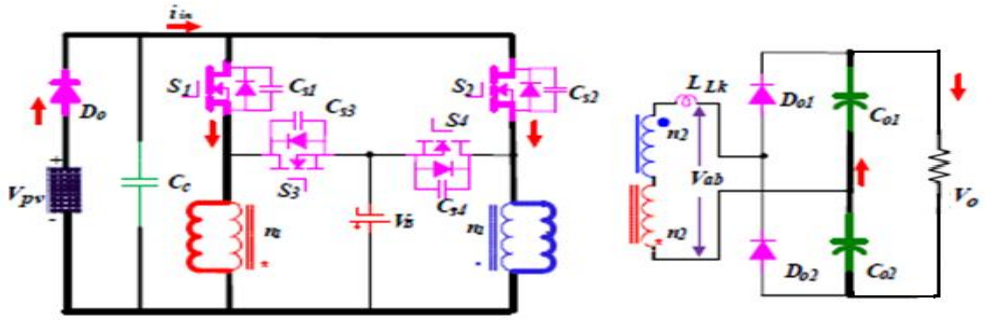

Figure 3.5: First operating states of the proposed converter with resistive load in mode 1

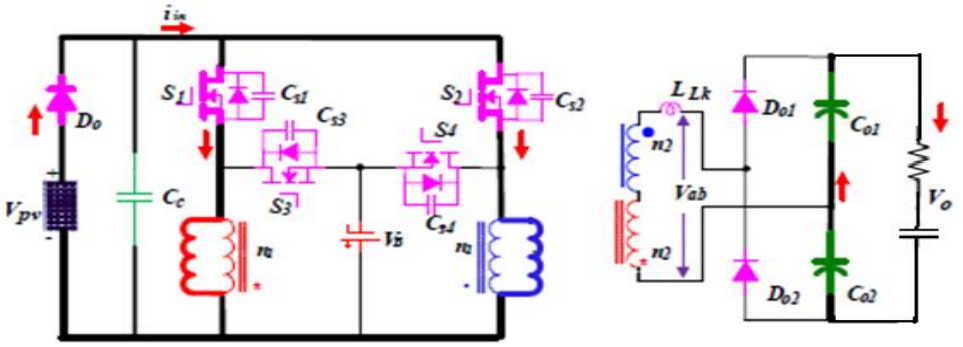

Figure 3.6: First operating states of the proposed converter with RC load in mode 1

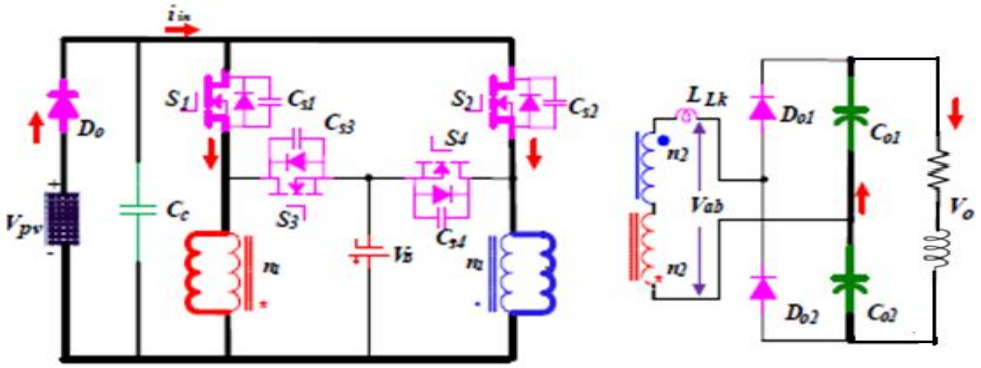

Figure 3.7: First operating states of the proposed converter with RL load in mode 1

State 2 [t_1-t_2]:

Att_1,$s_2$turns OFF, $s_4$turns ON, while the diodes $D_{01}$is ON. The primary side of the coupled inductor L_2charges the battery through s_4. During this state, L_1operates in the forward mode and L_2operates in the flyback mode to transfer energy to the load. When $s_1$turns on and $s_2$turns off, the primary voltage of the coupled inductor $L_1$is v_{pv} and the voltage on L_2 is $–V_B$.

According to the voltage balance law,

DV_{PV}= *(1-D)*V_B(3.1)

$V_{ab} = N\frac{1-D}{D}V_B - N(-V_B) = \frac{NV_B}{D}$(3.2)

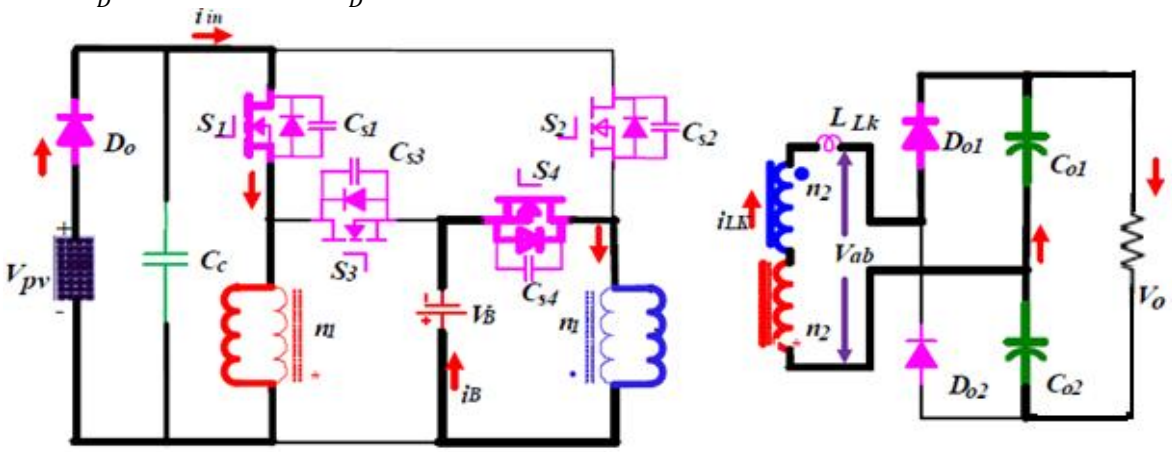

Figure 3.8: Second operating states of the proposed converter with resistive load in mode 1

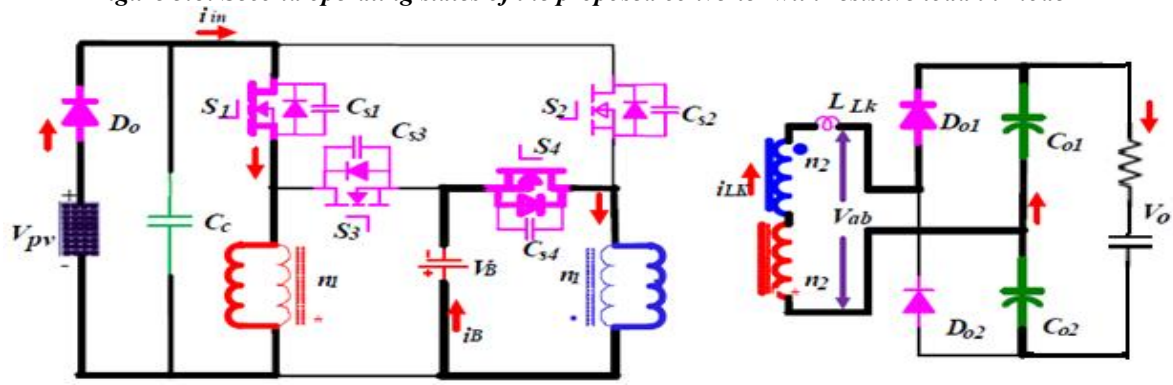

Figure 3.9: Second operating states of the proposed converter with RC load in mode 1

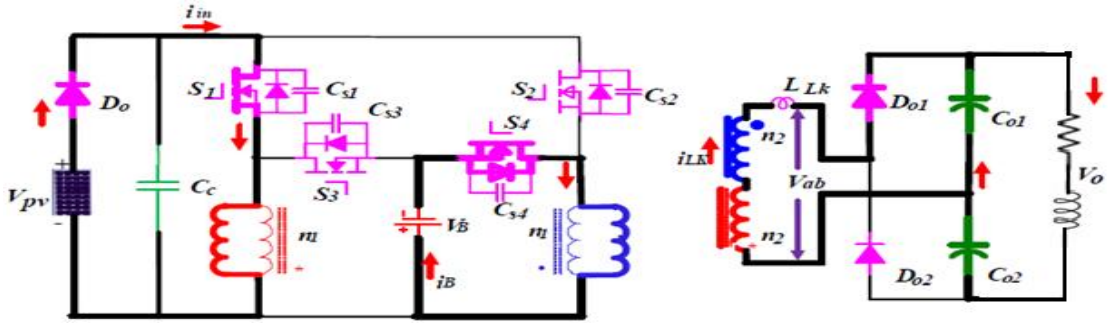

Figure 3.10 : Second operating states of the proposed converter with RL load in mode 1

State 3 [t_2-t_3]:

At t_2, s_2turns ON, it forces the two coupled inductors work in the flyback state to store energy and D_{02} is reverse-biased. The energy stored in $C_{01}$and C_{02}transfers to the load. Att_3, the leakage inductor current decreases to zero and the diode D_{01}turns OFF.

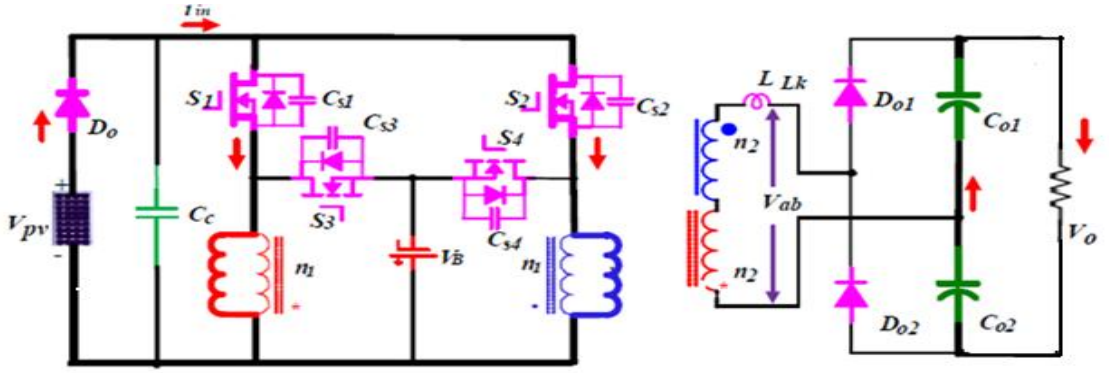

Figure 3.11: Third operating states of the proposed converter with resistive load in mode 1

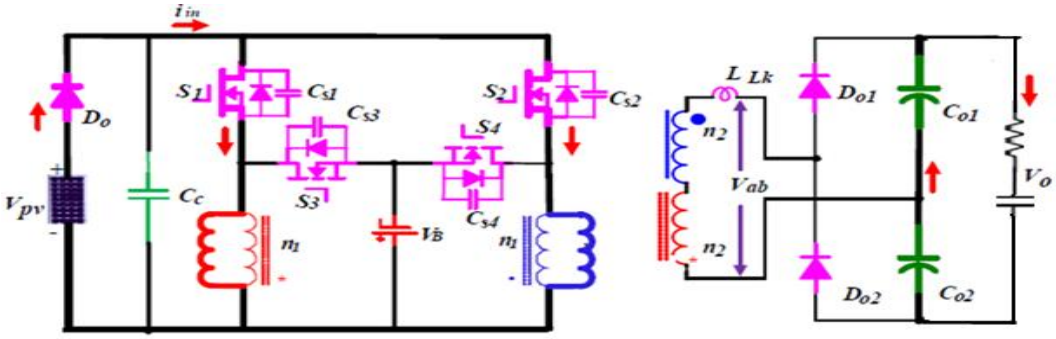

Figure 3.12: Third operating states of the proposed converter with RC load in mode 1

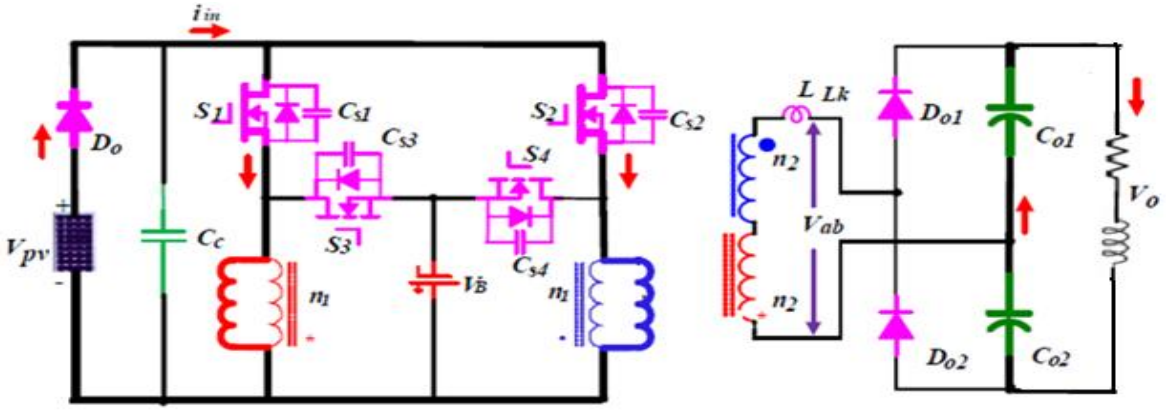

Figure 3.13: Third operating states of the proposed converter with RL load in mode 1

3.2 Performance Analysis And Feedback Loop Design

In order to realize flexible energy flow control, the modulation strategy is proposed to combine PWM with PS schemes. Firstly, the relationship of voltage gains with duty ratio and PS needs to be derived. In the following analysis, $s_1$and $s_2$have the same duty ratio *D,* whilst $s_3$and $s_4$share another duty ratio. The gate signals for $s_1$and $s_3$are complementary, and so are $s_2$and s_4.

3.3.1 Analysis of Circuit Performance for D≥0.5

When the duty cycle D≥0.5, there are five operating cases which need to be analyzed, as shown in Fig. 9.

In case 1, the phase shift angle is between *0* and φ_{crit1}. From the waveform of the leakage inductor current, the secondary side of the coupled inductor is equivalent to a discontinuous conduction mode (DCM) of a Buck converter.

$$\frac{NV_B}{D}.\frac{\varphi_{crit1}}{2\pi}.T_s = \frac{V_0}{2}(1 - D - \frac{\varphi_{crit1}}{2\pi})T_s (3.3)$$

$$\varphi_{crit1} = \pi.D.(1 - D).\frac{V_{out}}{N.V_B} (3.4)$$

The secondary side of the coupled inductor is equivalent to two Buck converters connected in parallel at the DCM operational condition. The corresponding equivalent duty ratio of the Buck converter is $\varphi/2\pi$.

Provided the voltage gain of the Buck converter in DCM, the output voltage is given by:

$$V_0 = 2.\frac{2}{1+\sqrt{1+\frac{4.2L_k}{R_0.T_S.(\varphi/2\pi)^2/2}}} (3.5)$$

In case 2, the phase shift angle is between$\varphi_{crit1} and\ \varphi_{crit2}$. φ_{crit2}, is the transition point from a continuous conduction mode (CCM) to a DCM, which can be determined by Eq 3.6. The voltage equations at $\varphi_{crit1}$and $\varphi_{crit1}$are derived by Eqs 3.7 and 3.8.

$$\varphi_{crit2} = \frac{4\pi.(1-D)}{D}.\frac{N.V_B}{V_{out}} (3.6)$$

$$\frac{NV_B}{DL_k}(1 - D) = \frac{V_0}{2L_k}\frac{\varphi_{crit2}}{2\pi} (3.7)$$

$$\frac{NV_B}{DL_k}\frac{\varphi_{crit2}}{2\pi} = \frac{V_0}{2L_k} (1-D) (3.8)$$

3.3.2 Analysis of Circuit Performance for D<0.5

Similarly, there are five operating cases for *D*<0.5.

In Case 1 ($0<\varphi<\varphi_{crit1}$), considering the waveform of the leakage inductor current, the secondary side of the coupled inductor is equivalent to a DCM Buck converter, the corresponding duty ratio is $D=\varphi/2\pi$. Thus the critical angle and the output voltage are:

$$\varphi_{crit1} = \pi.D^2.\frac{V_0}{N.V_B} (3.15)$$

$$V_0 = 2.\frac{2}{1+\sqrt{1+\frac{4.2L_k}{R_0.T_S.(\varphi/2\pi)^2/2}}}.\frac{NV_B}{D} (3.16)$$

In case 2 (φ_{crit1}), $<\varphi<\varphi_{crit2}$),), the leakage inductor current is still above zero. The system equations can be expressed as,

$$\varphi_{crit2} = 4\pi.\frac{N.V_B}{V_0} (3.17)$$

$$\frac{NV_B}{DL_k}.\frac{\varphi_{crit1}}{2\pi} = \frac{V_0}{2L_k}.D (3.18)$$

$$\frac{NV_B}{DL_k}.\ D = \frac{V_0}{2L_k}.\frac{\varphi_{crit2}}{2\pi} (3.19)$$

In case 3 ($\varphi_{crit2}<\varphi<\varphi_{crit3}$), the duty ratio of the secondary winding is equal to *D*. The system equations are,

$$\varphi_{crit3} = 2\pi - \varphi_{crit2} (3.20)$$

$$\frac{NV_B}{DL_k}.\ D = \frac{V_0}{2L_k}(1 - \frac{\varphi_{crit3}}{2\pi}) (3.21)$$

$$V_0 = 2.\frac{2}{1+\sqrt{1+\frac{4.2L_k}{R_0.T_S.(D)^2/2}}}.\frac{NV_B}{D} (3.22)$$

In case 4 ($\varphi_{crit3}<\varphi<\varphi_{crit4}$), the leakage inductor current is still above zero. The system equations can be expressed as,

$$\varphi_{crit4} = 2\pi - \varphi_{crit1} (3.23)$$

$$\frac{NV_B}{DL_k}.\left(1 - \frac{\varphi_{crit4}}{2\pi}\right) = \frac{V_0}{2L_k}.D (3.24)$$

In case 5 ($\varphi_{crit4}<\varphi<2\pi$), the duty ratio of the secondary winding is *1-*$\varphi/2\pi$. The output voltage is derived by,

$$V_0 = 2.\frac{2}{1+\sqrt{1+\frac{4.2L_k}{R_0.T_s.(1-\varphi/2\pi)^2/2}}}.\frac{NV_B}{D}(3.25)$$

From the above derivations, D is the control variable to balance the PV voltage and battery voltage and φ is employed to control the secondary output voltage. The two-freedom control makes it flexible to control the PV, battery and load. One condition should be applied to achieve decoupled control, performance, which can be expressed as $0<\varphi<\varphi_{crit2}$ and $\varphi_{crit3}<\varphi<2\pi$. If this is not satisfied, the secondary output voltage is dictated by the switching duty cycle instead of the phase shift angle as presented in Eqs. 3.11 and 3. 22.

3.2.1 Design Considerations

In the MPPT control, the PV energy transfers to the battery, the circuit is a Buck-Boost converter. The maximum load voltage at idea conditions can be expressed as,

$$V_{0(\max)} = \frac{2N}{D}V_B \ (3.26)$$

In order to realize the decoupling of load voltage and MPPT control, the output voltage (in Eq 3.26)should be larger than the reference load voltage to gain a large phase shift angle.

Design considerations can be listed as follows: (i) Confirm PV array MPP voltage and corresponding control region and battery; Calculate D working region. (ii) Choose the turns ratio of the coupled inductor to guarantee a large phase shift angle, following Eq 3. 27.

$$N=\frac{V_{0_{aim}}(1+\alpha)}{2V_B}D(3.27)$$

Where, α is the phase shift angle coefficient, and $V_{0_aim}$is the reference output voltage. Fig3.13 illustrates a design case study for a 16 V (open voltage) PV module with 12 V battery voltages and 80 V reference output voltages. In this case, by choosing 2 as the coupled inductor turns ratio, a phase shift control margin of at least 18 V can be achieved.

3.3 Matlab Tools And Usage

3.3.1 Introduction

MATLAB is a multi-paradigm numerical computing environment and fourth-generation programming language. Developed by Math Works, MATLAB allows matrix manipulations, plotting of functions and data, implementation of algorithms, creation of user interfaces, and interfacing with programs written in other languages, including C, C++, Java, Fortran and Python. Although MATLAB is intended primarily for numerical computing, an optional toolbox uses the MuPAD symbolic engine, allowing access to symbolic computing capabilities. In 2004, MATLAB had around one million users across industry and academia. MATLAB users come from various backgrounds of engineering, science, and economics. MATLAB is widely used in academic and research institutions as well as industrial enterprises. MATLAB is a high-performance language for technical computing. It integrates computation, visualization, and programming in an easy-to-use environment where problems and solutions are expressed in familiar mathematical notation.

Typical uses include:

- Math and computation
- Algorithm development
- Modeling, simulation, and prototyping
- Data analysis, exploration, and visualization

3.3.2 Key Features

- High-level language for numerical computation, visualization, and application development
- Interactive environment for iterative exploration, design, and problem solving.
- Mathematical functions for linear algebra, statistics, Fourier analysis, filtering, optimization, numerical integration, and solving ordinary differential equations.

4 SIMULATION RESULTS

4.1 Simulink Diagram

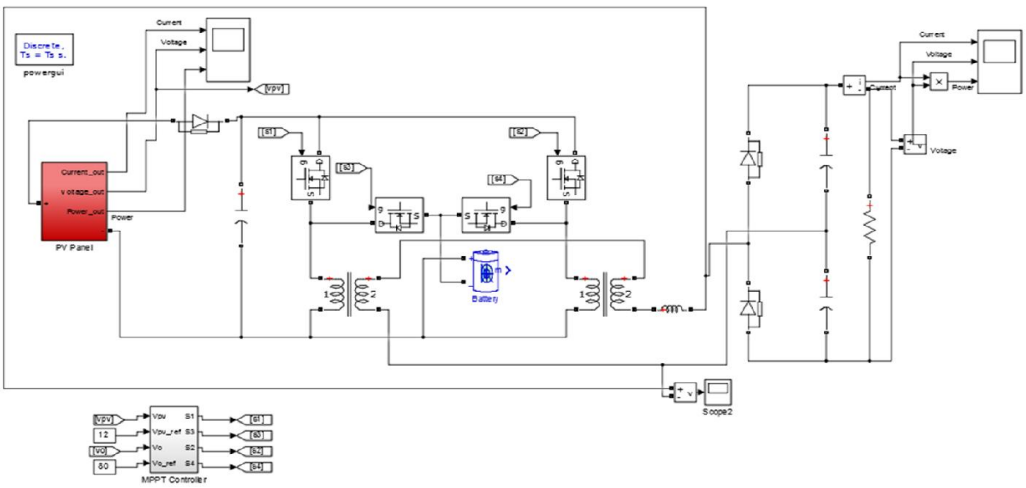

Figure 4.1: Simulink diagram of threeport converter with resistive load

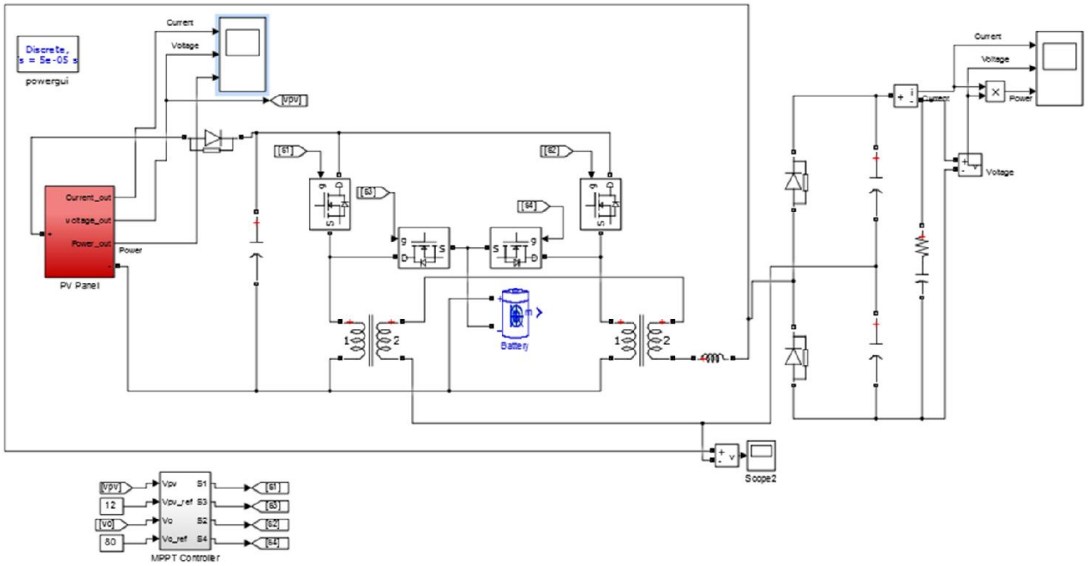

Figure 4.2: Simulink diagram of threeport converter with RC load

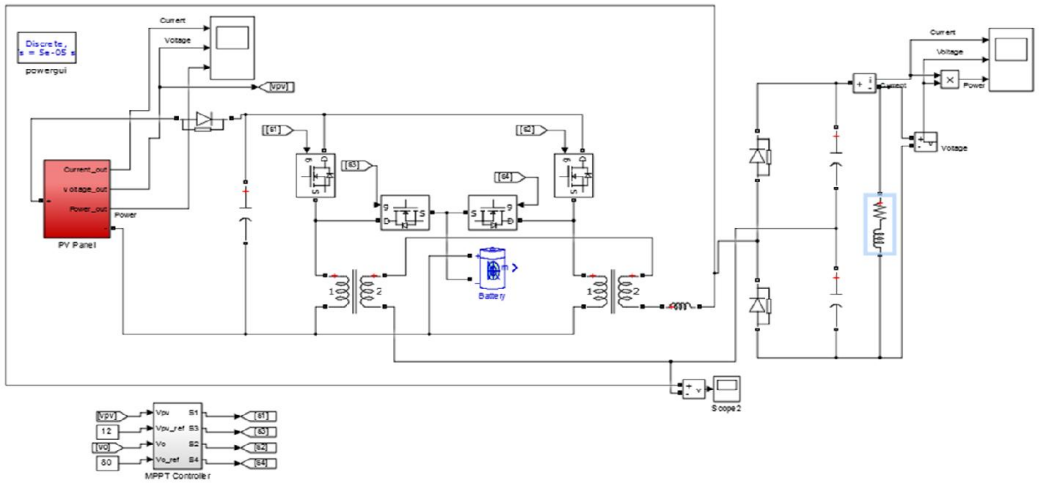

Figure 4.3: Simulink diagram of three port converter with RL load

4.2 Solar Panel

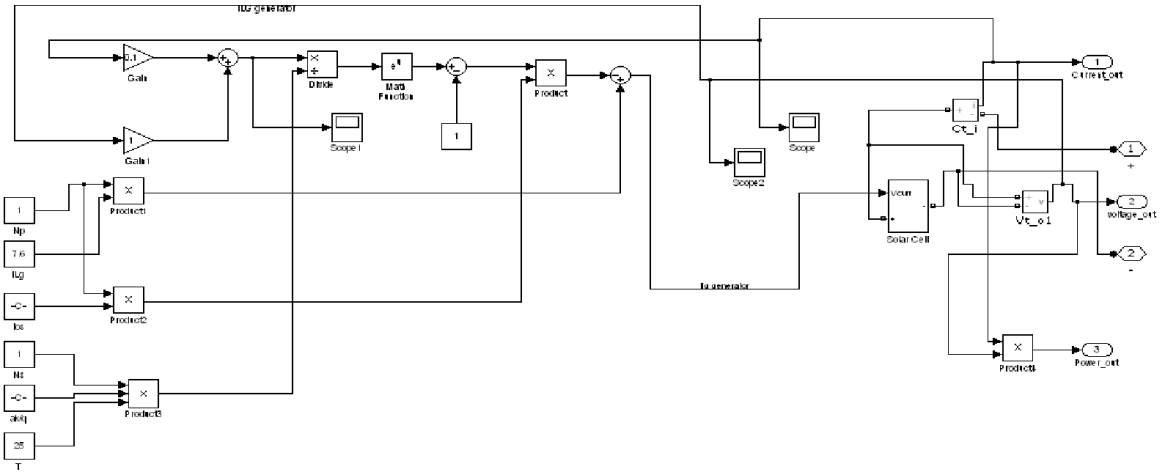

Figure 4.4: Simulink diagram of PV panel

4.3 Simulation Output

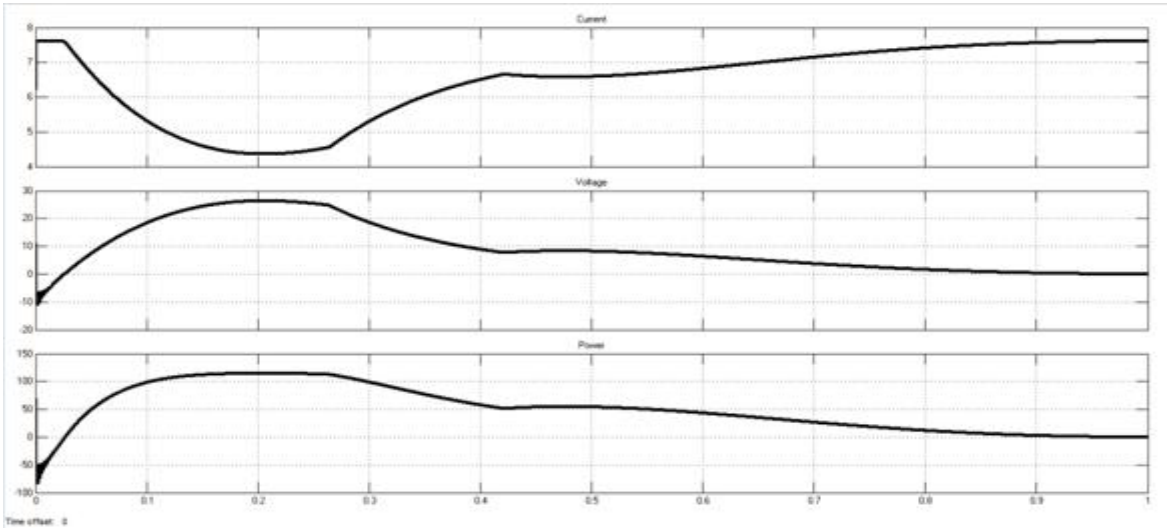

Figure 4.5: Input waveform of three port converter with resistive load

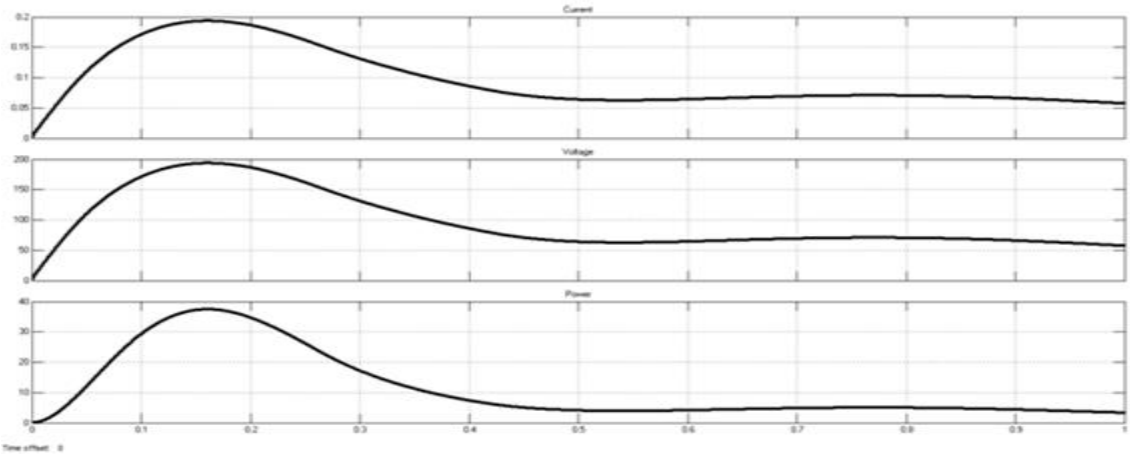

Figure 4.6: Output waveform of three port converter with resistive load

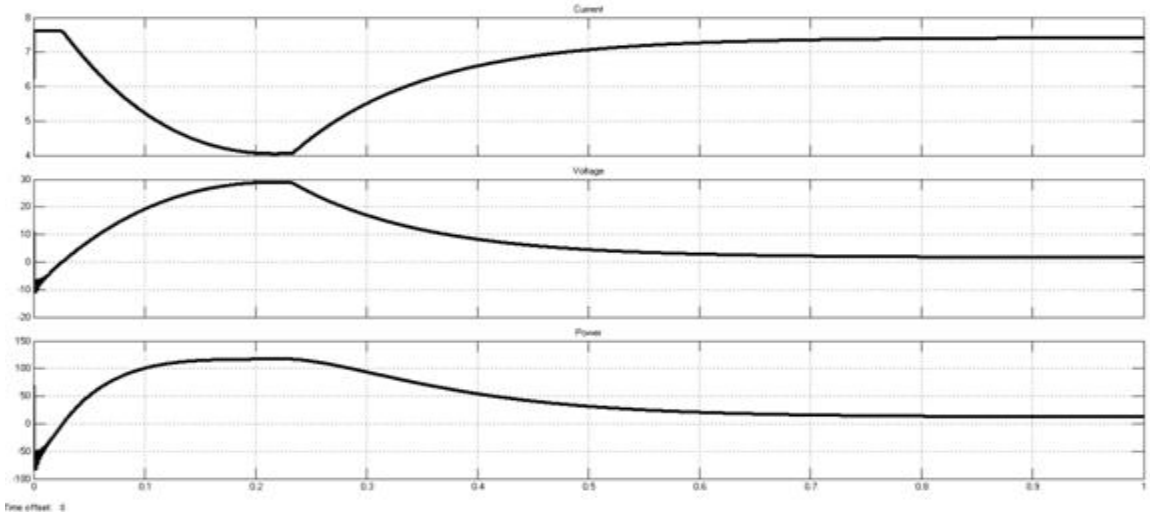

Figure 4.7: Input waveform of three port converter with RC load

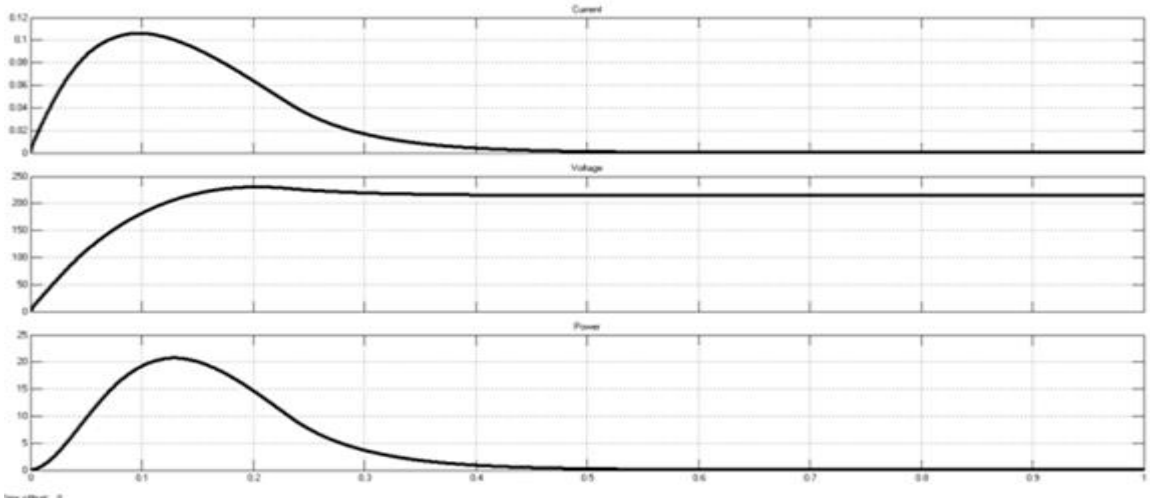

Figure 4.8 : Output waveform of three port converter with RC load

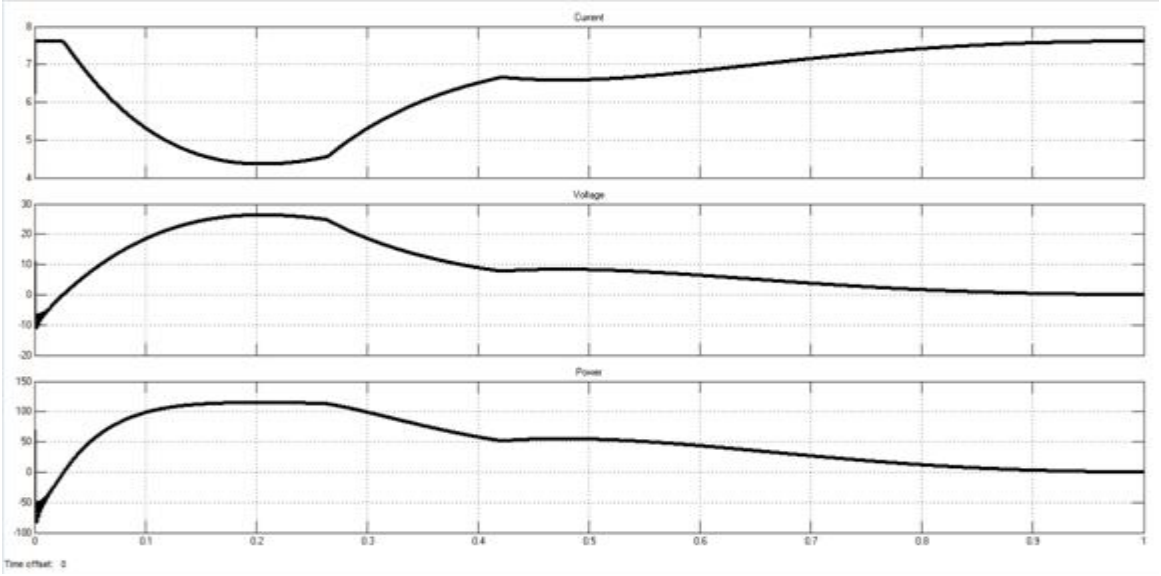

Figure 4.9 : Input waveform of three port converter with RL load

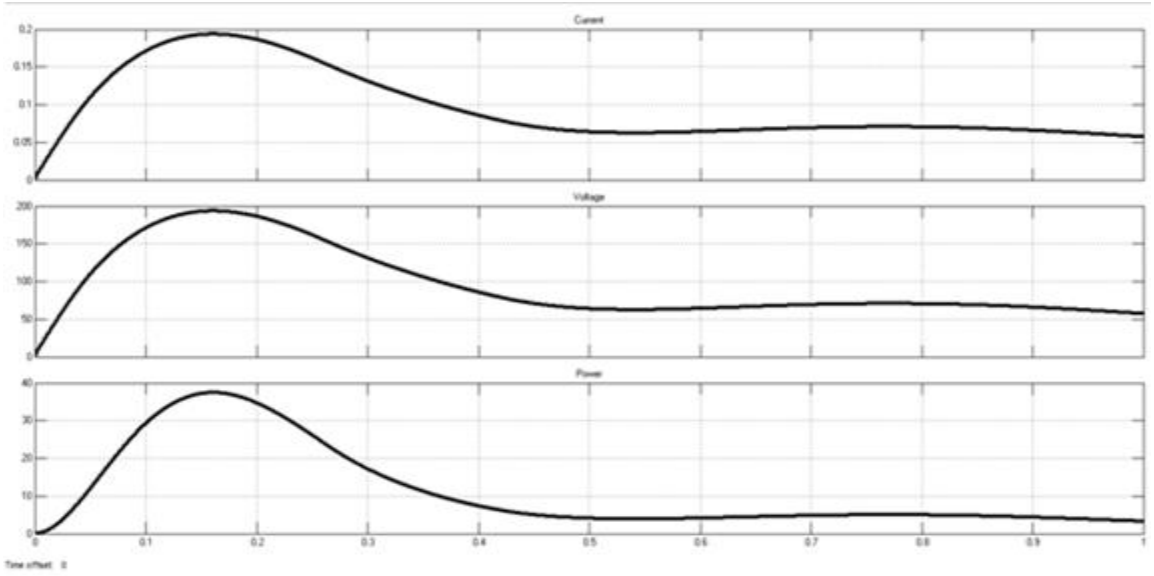

Figure 4.10 : Output waveform of three port converter with RL load

4.4 Output Comparision

i. In resistive load, the current through the resistor is directly proportional to the potential difference across it.
ii. In RC circuit, the voltage supply initially causes a current as it accumulates charge, this current will however decay in time as the capacitor fills, eventually falling to zero. A capacitor will therefore not permit a steady state current to pass.
iii. The RL circuit will freely allow an unchanging current but opposes a rapidly changing one.

5 CONCLUSION

An isolated three-port DC-DC converter for stand-alone PV systems, based on an improved Flyback-Forward topology is proposed. The converter can provide a high step-up capability for power conversion systems including the PV array, the battery storage, and the isolated load consumption. Three operating modes are analyzed and have shown the effective operation of the proposed topology for PV applications. From simulation and experimental tests, it can be seen that the output voltage and PV voltage can be controlled independently by the phase angle shift and PWM, respectively. The decoupled control approach is a simple but effective way to achieve the regulation of output voltage and PV voltage, which is important for MPPT of stand-alone PV systems. In addition, a 250 W converter is prototyped and tested to verify the effectiveness of the proposed converter topology and control scheme. The developed technology is capable of achieving MPPT, high conversion ratio and multiple operating modes whist still making the converter relatively simple, light, efficient and cost-effective.

REFERENCES

[1] K. Basu, N. Mohan, "A high-frequency link single-stage PWM inverter with common-mode voltage suppression and source-based commutation of leakage energy," IEEE Trans. Power Electron., vol. 28, no. 8, pp. 3907-3918, Oct. 2014.
[2] C. Konstantopoulos, E. Koutroulis, "Global maximum power point tracking of flexible photovoltaic modules," IEEE Trans. Power Electron., vol. 29, no. 6, pp. 2817-2828, Oct. 2014.
[3] W. Li, W. Li, X. Xiang, Y. Hu, X. He, "High step-up interleaved converter with built-in transformer voltage multiplier cells for sustainable energy applications," IEEE Trans. Power Electron., vol. 29, no. 6, pp. 2829-2836, Jun. 2014.

[4] Y. Hu, Y. Deng, Q. Liu, X. He, "Asymmetry three-level grid-connected current hysteresis control with varying bus voltage and virtual over-sample method," IEEE Trans. Power Electron.vol. 29, no. 6, pp. 3214-3222, Jun. 2014.
[5] F. Nejabatkhah, S. Danyali, S. H. Hosseini, M. Sabahi,and S. M. Niapour, "Modeling and control of a new three-input DC-DC boost converter for hybrid PV/FC/battery power system," IEEE Trans. Power Electron., vol. 28, no. 10, pp. 4612-4624, Oct. 2013.
[6] F. Zhang, K. Thanapalan, A. Procter, S. Carr, J. Maddy, "Adaptive Hybrid Maximum Power Point Tracking Method for a Photovoltaic System," IEEE Trans. Energy Conversion, vol. 28, no. 2, pp. 353-360, June 2013.
[7] P. Thounthong, "Model Based-Energy Control of a Solar Power Plant With a Supercapacitor for Grid-Independent Applications," IEEE Trans. Energy Conversion, vol. 26, no. 4, pp. 1210-1218, 2011.
[8] A. Elmitwally, M. Rashed, "Flexible Operation Strategy for an Isolated PV-Diesel MicrogridWithout Energy Storage," IEEE Trans. Energy Conversion, vol. 26, no. 1, pp. 235-244, 2011.
[9] J. K. Shiau, D. M. Ma, P. Y. Yang, G. F. Wang, and J. H. Gong, "Design of a Solar Power Management System for an Experimental UAV," IEEE Trans. Aerospace and Electronic Systems, vol. 45, no. 4, pp. 1350-1360, Oct. 2009.
[10] F. S. Kang, S. J. Park, S. E. Cho, C. U. Kim, T. Ise, "Multilevel PWM inverters suitable for the use of stand-alone photovoltaic power systems," IEEE Trans. Energy Conversion, vol. 20, no. 4 , pp. 906-915, 2005.
[11] H. Valderrama-Blavi, J. M. Bosque, F. Guinjoan, L. Marroyo, and L. Martinez-Salamero, "Power Adaptor Device for Domestic DC Microgrids Based on Commercial MPPT Inverters," IEEE Trans. Ind. Electron., vol. 60, no. 3, pp. 1191-1203, Mar. 2013.
[12] H. Wu, K. Sun, R. Chen, H. Hu, and Y. Xing, "Full-Bridge Three-Port Converters With Wide Input Voltage Range for Renewable Power Systems," IEEE Trans. Power Electron., vol. 27, no. 9, pp. 3965-3974, Sept. 2012.
[13] O. Elma, and U. S. Selamogullari, "A comparative sizing analysis of a renewable energy supplied stand-alone house considering both demand side and source side dynamics," Applied Energy, vol. 96, pp. 400-408, 2012.
[14] H. Wu, R. Chen, J. Zhang, Y. Xing, H. Hu, and H. Ge, "A Family of Three-Port Half-Bridge Converters for a Stand-Alone Renewable Power System," IEEE Trans. Power Electron., vol. 26, no. 9, pp. 2697-2706, Sept. 2011.